Bull Earthquake Eng (2009) 7:343–361
DOI 10.1007/s10518-009-9103-z

ORIGINAL RESEARCH PAPER

Assessment and modeling of embankment participation in the seismic response of integral abutment bridges

A. N. Kotsoglou · S. J. Pantazopoulou

Received: 13 December 2007 / Accepted: 19 January 2009 / Published online: 4 February 2009

Abstract The dynamic response and seismic performance of bridges may be appreciably affected by numerous contributing factors, with soil–structure interaction being the dominant exogenous influence. The most familiar form is the so-called soil–pile interaction, but embankment–abutment interaction is also documented through field observations and analytical investigations, particularly evident in integral R.C. bridges. Recent studies have shown that this form of interaction may significantly alter the bridge response and should be taken into account during design and assessment, especially in the case of typical highway overcrossings that have abutments supported on earth embankments. In light of this emerging problem and in order to facilitate quantitative estimates of the interaction effects, the question of appropriate modeling and seismic assessment of R.C. integral bridges is the main object of the present paper. Based on already established procedures to account for soil–structure interaction, a new approach is proposed to model the contribution of the embankment, the bent and the abutments to the overall bridge response. Furthermore, the capacity curve of the entire bridge system is evaluated through the implementation of Incremental Dynamic Analysis (IDA), therefore allowing for seismic assessment of the complex superstructure–foundation system with well established displacement based procedures. Using as a benchmark case two typical instrumented U.S. highway bridges located in California, the proposed method is implemented and provided results from this analysis are correlated successfully with available field data. Results obtained from the analysis indicate excessive displacement demands for the entire bridge–embankment system owing to the embankment contribution and the soil degradation under increasing shear strains. Furthermore, seismic performance is strongly related to the central bent deformation capacity, with soil–pile interaction effects being of critical importance.

A. N. Kotsoglou (✉) · S. J. Pantazopoulou
Department of Civil Engineering, Laboratory of Reinforced Concrete, Democritus University of Thrace, V. Sofias 12, Xanthi 67100, Greece
e-mail: akotsogl@civil.duth.gr

S. J. Pantazopoulou
e-mail: pantaz@civil.duth.gr

Keywords Highway overcrossings · Soil–structure interaction · Embankment flexibility · Seismic response

List of symbols

$u(x, y)$	Embankment displacements as a function of x and y coordinates
$\rho, G(z)$	Soil density and Soil shear modulus as a function of depth z
B_c, L_c	Effective Embankment Crest Width, Embankment Critical Length
H, L	Embankment Height, Embankment Length
f_s, D	Pile skin resistance, Pile diameter
x, y, z	Transverse, Longitudinal and Vertical axes (Embankment model)
$\Phi(y, z)$	Deformation shape as a function of y and z coordinates (Embankment model)
$M^*_{\text{tot}}, K^*_{\text{tot}}, C^*_{\text{tot}}$	Generalized mass, Stiffness and Damping Coefficient (for the generalized SDOF representation of the Embankment)
$\Im^*_{\text{tot}}, \xi$	Generalized system excitation factor, damping ratio of the consistently-linearized Embankment model
$Y(t)$	A time dependent generalized coordinate (Embankment model)
u_g	Imposed ground displacements
$M_{\text{center}}, M_{\text{edge}}$	Deck mass (center), Deck mass (edge) (Deck–pier–abutment substructure model)
$M_{\text{emb}}, C_{\text{emb}}$	Embankment lumped mass attached on the deck, lumped damper property attached on the deck to represent the embankment contribution (Deck–pier–abutment substructure model)
$K_{\text{deck}}, K_{\text{bent}}, K_{\text{abut}} K_{\text{emb}}$	Deck stiffness, Bent stiffness, Abutment stiffness and Embankment stiffness contributions to the deck–pier–abutment substructure model.
$u_{\text{tot}}, u_1, \alpha_1$	Total transverse displacements, Bent relative transverse displacements, Bent–abutment displacement ratio
u_y, u_D, μ_d	Apparent Yield Displacement, Displacement Demand, Displacement ductility (bridge–embankment system)
$p_l, p^h_{s,\text{vol}}, P/A_g f_c$	Longitudinal reinforcement ratio, transverse volumetric steel ratio of the column cross-section, axial load ratio.

1 Introduction

Appropriate modeling and seismic assessment of typical integral highway overcrossings are the main issues investigated in this paper, with particular emphasis on the modification of dynamic response effected by the supporting soil conditions and soil–superstructure interaction (Priestley et al. 1996; Mackie and Stojadinovic 2003; Kappos et al. 2007). Clearly, stiff soil conditions are approximated adequately by the assumption of fixed bridge supports; such an assumption would be realistic in the case of small intensity excitations. However,

due to the propensity of the soil to undergo stiffness degradation under increasing deformation, soil compliance becomes increasingly important with the intensity of seismic demand. Therefore, in order to obtain a consistent representation of bridge response to a wide range of imposed ground excitation intensities, it is important to account for the significance of soil–pile and abutment–embankment interaction in an expanded bridge deck–pier–abutment superstructure model. Of these two types of interaction, the embankment–abutment interaction has received attention only recently; here the soil mass is considered to interact inertially and kinematically with the entire system (deck–pile foundation–abutments–bents) and this kind of interaction may have significant effects especially during strong intensity ground-excitations.

A few simplified models have been used to approximate the dynamic response of highway overcrossings when accounting for embankment–bridge interaction. The basis for most of these approaches has been the so-called "shear wedge" approximation for the approach embankment (Wilson and Tan 1990a,b; Wissawapaisal 1999; Inel 2001; Inel and Aschheim 2004). In order to approximate the embankment mobilization with a lengthwise uniform shear wedge in these studies, values of "embankment effective length-L_{eff}" were identified through correlation of analysis results with recorded responses. Zhang and Makris (2001, 2002a,b) also investigated the problem and proposed simplified stick models for the estimation of the seismic response of highway overcrossings based on a one dimensional analytical model for the approach embankments (Gazetas 1987). Springs and dashpots were attached on the bridge deck to simulate the bent and abutment contribution to the response of the entire system. Values of "embankment critical length-L_c" were provided by a derived closed form relationship, dependent only on the embankment cross-sectional geometry. Factors contributing to bridge–embankment interaction were also studied by Price and Eberhard (1998) who proposed a modeling method based on detailed 3D equivalent elastic analysis. Other studies quantified the embankment contribution through various identification procedures from the recorded field data of instrumented bridges (McCallen and Romstad 1994; Goel and Chopra 1997).

Clearly, bridge–embankment interaction is a problem of considerable complexity. Despite the notable number of models published in this field, a pressing need still remains for a general procedure applicable to a wide range of bridge systems and soil conditions. The basis for development of a generalized procedure lies in the solution of the field equations of the embankment's dynamic response (Kotsoglou and Pantazopoulou 2007a). To use this solution in the context of an overall bridge model, bridge–embankment inertial and kinematic interaction was simulated through appropriate masses, springs and dashpots (to account also for the increased energy dissipation of the soil mass owing to its hysteresis), whereas the embankment contribution to the bridge response was quantified explicitly through the critical length evaluation based on the derived field equations, given as a function of many contributing factors (i.e. imposed boundary conditions, soil shear modulus, and embankment geometry). In implementing the proposed two dimensional modeling approach, there is no requirement for prior knowledge of any participating factor that may contribute to the overall dynamic response of the system.

Using this general approach to quantify soil–structure interaction and embankment mobilization, the present paper is focused on assessment and design guidance for highway overcrossings. The capacity curve of the entire system is established through Incremental Dynamic Analysis (I.D.A., Vamvatsikos and Cornell 2004), in order to account for the dependence of the system's dynamic characteristics on the magnitude of shear deformation as induced by ground excitations of different intensity. Seismic assessment and design of highway overcrossings is based on a simplified ESDOF representation in conjunction with

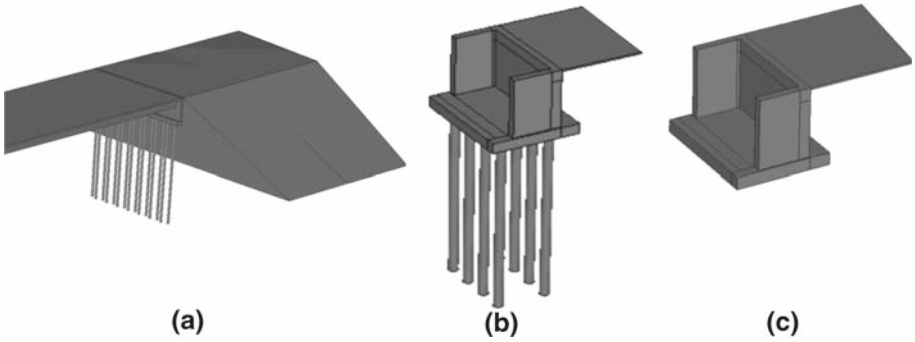

Fig. 1 **a** Bridge abutment supported on earth embankment (assembly), **b** Stiff bridge abutment and **c** Abutment on shallow foundation

acceleration-displacement response spectra. The proposed assessment and design method is implemented in the case of two well documented and instrumented integral bridges under a wide range of earthquake records. The analysis results show that a significant degree of nonlinearity, evident in the overall response of the system, is owing to the bridge–embankment interaction and the progressive embankment-soil shear-modulus degradation. In the case studies considered, in light of the imposed excessive displacement demands, the capability of the central bent columns to undertake successfully the superstructure loads is strongly dependent on the soil foundation properties and soil–pile interaction effects.

2 Seismic assessment of highway overcrossings

The model bridge structure considered in the present paper is a typical highway overcrossing with abutments supported on approach embankments through a flexible pile foundation (typical of US highway construction, Fig. 1a). Owing to soil nonlinearity, embankments exhibit increasingly compliant performance under high shear deformation levels and therefore soil displacements at bridge abutment supports may be significant, particularly in the transverse direction. At that stage, the integral superstructure is driven almost as a rigid body by the embankment motion (Inel 2001). This response drives also the central bent piers which undergo significant deformation demands. The type of response described is less prevalent in the European typical bridge structure, where usually stiff abutments supported on stiff, large diameter piles are constructed. Nevertheless, even in these cases, inertial and kinematic bridge–embankment interaction can still become significant, the more so in the longitudinal direction of the bridge. Appreciable soil–structure interaction is expected in case of abutments founded on large pilecaps due to mobilization of the supporting soil (Fig. 1b) but also in case of flexible shallow foundations (Fig. 1c) where embankment inertial and kinematic contributions to the overall response become significant as the foundation flexibility increases.

3 Bridge–embankment interaction under transverse ground excitation

In the proposed approach, the bridge–embankment system is idealized as a series of substructure models which are interacting at the contact degrees of freedom (Fig. 2). In each of these

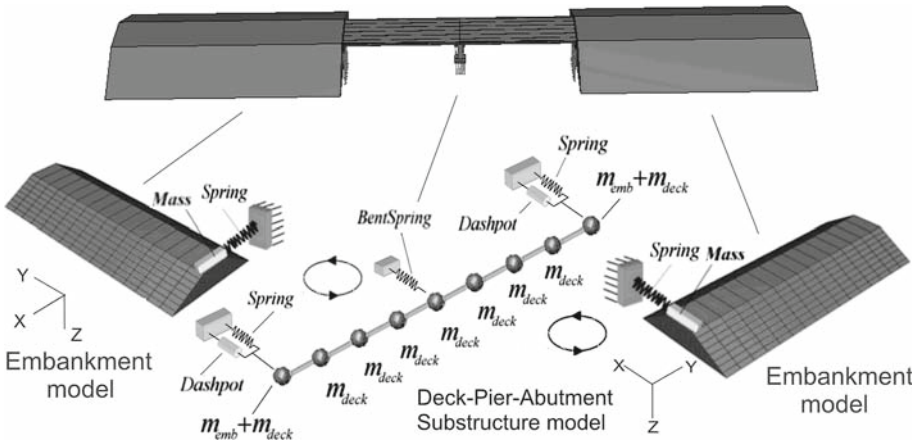

Fig. 2 Simplified deck–pier–abutment substructure and embankment models

models, the effect of the adjacent interacting substructure is represented through lumped masses, springs and dashpots attached at the point of contact. In the case of the embankment model, the lumped properties represent the contribution of the deck–bent–abutment substructure, whereas in the case of the deck–bent–abutment model, the lumped properties represent the contribution of the embankment substructures (to the left and right of the bridge).

For the embankment substructure, explicit analytical solutions are provided based on the two dimensional analytical model originally developed from first principles (Kotsoglou and Pantazopoulou 2007a). According to the model, the equation of motion of the embankment is:

$$-\rho \cdot \ddot{u}_{\text{tot}} + \frac{\mathrm{d}}{\mathrm{d}z}\left(G(z) \cdot \frac{\mathrm{d}u}{\mathrm{d}z}\right) + \frac{\mathrm{d}}{\mathrm{d}y}\left(G(z) \cdot \frac{\mathrm{d}u}{\mathrm{d}y}\right) = 0 \tag{1}$$

The above is reduced to the response of an ESDOF system vibrating in a single mode, which here is approximated by the fundamental mode of vibration of the embankment, $\Phi(y, z)$. In the embankment model, properties of the lumped elements at the contact node are estimated from the deck–pier–abutment substructure model. For this purpose, a set of three degrees of freedom are considered on the deck: u_1 is the transverse displacement at the center of mass, and u_2, u_2' the transverse displacements at the points of contact with the embankment, taken here proportional to u_1 through coefficient a_1 (i.e.,$u_2 = a_1 \cdot u_1$), (Fig. 3). With reference to the simplified embankment model shown in Fig. 2, and after consideration of the boundary conditions imposed by the bridge (Fig. 3), the general equation of motion for the bridge–embankment system is provided through virtual work analysis:

$$\begin{aligned} &1/2M_{\text{center}} \cdot \ddot{u}_{\text{tot},1} + a_1 \cdot (M_{\text{edge}} + M_{\text{emb}}) \cdot \ddot{u}_{\text{tot},2} + C_{\text{emb}} \cdot a_1^2 \cdot \dot{u}_1 + 1/2K_{\text{bent}} \cdot u_1 \\ &\quad + a_1^2 \cdot (K_{\text{emb}} + K_{\text{abut}}) \cdot u_1 + K_{\text{deck}} \cdot u_1 \cdot (1 - a_1)^2 = 0 \end{aligned}$$

which is further expanded to:

$$\begin{aligned} &1/2M_{\text{center}} \cdot (\ddot{u}_1 + \ddot{u}_g) + (M_{\text{edge}} + M_{\text{emb}}) \cdot (a_1^2 \cdot \ddot{u}_1 + \alpha_1 \cdot \ddot{u}_g) + C_{\text{emb}} \cdot a_1^2 \cdot \dot{u}_1 \\ &\quad + 1/2K_{\text{bent}} \cdot u_1 + (K_{\text{emb}} + K_{\text{abut}}) \cdot \alpha_1^2 \cdot u_1 + K_{\text{deck}} \cdot u_1 \cdot (1 - a_1)^2 = 0 \end{aligned}$$

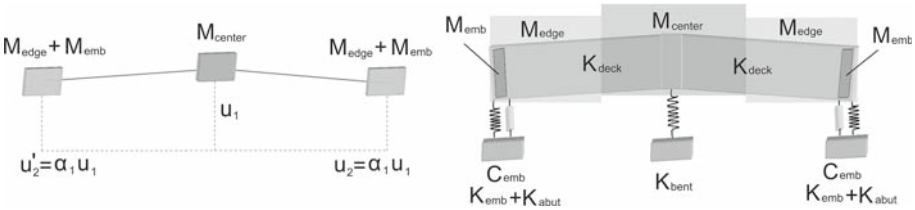

Fig. 3 Simplified deck model

Thus, to approximate the complex bridge response through the response of its center of deck mass, the following generalized SDOF equation of motion need be solved in time:

$$\begin{aligned}&[1/2M_{\text{center}} + \alpha_1^2 \cdot (M_{\text{edge}} + M_{\text{emb}})] \cdot \ddot{u}_1 + C_{\text{emb}} \cdot a_1^2 \cdot \dot{u}_1 \\ &\quad + [1/2K_{\text{bent}} + \alpha_1^2 \cdot (K_{\text{emb}} + K_{\text{abut}}) + (1 - a_1)^2 K_{\text{deck}}] \cdot u_1 \\ &= -[1/2M_{\text{center}} + a_1 \cdot (M_{\text{edge}} + M_{\text{emb}})] \cdot \ddot{u}_g \end{aligned} \tag{2}$$

From (2) and assuming the case of uniform displacement distribution along the deck ($a_1 = 1$, as is usually observed in short bridges with symmetric spans), the contributing dynamic properties of the superstructure are carried over in equal amounts to both embankments (Eq. 3):

$$\begin{aligned}&[1/2M_{\text{center}} + M_{\text{edge}} + M_{\text{emb}}] \cdot \ddot{u}_1 + C_{\text{emb}} \cdot \dot{u}_1 + [1/2K_{\text{bent}} + K_{\text{emb}} + K_{\text{abut}}] \cdot u_1 \\ &= -[1/2M_{\text{center}} + M_{\text{edge}} + M_{\text{emb}}] \cdot \ddot{u}_g \end{aligned} \tag{3}$$

Based on the general case study (Eq. 2) and selecting the central bent coordinate as a reference point, dynamic characteristics of the embankment model of Fig. 2 are provided in (4):

$$\begin{aligned} M^*_{\text{tot}} &= 1/2M_{\text{center}} + \alpha_1^2 \cdot (M_{\text{edge}} + M_{\text{emb}}) = 1/2M_{\text{center}} \\ &\quad + a_1^2 \cdot \left(M_{\text{edge}} + B_c \cdot \int_0^{L_c} \int_0^{H} \rho \cdot \Phi^2(z, y) \cdot \mathrm{d}z \cdot \mathrm{d}y \right) \end{aligned} \tag{4a}$$

$$\begin{aligned} \Im^*_{\text{tot}} &= [1/2M_{\text{center}} + a_1 \cdot (M_{\text{edge}} + M_{\text{emb}})] = 1/2M_{\text{center}} \\ &\quad + a_1 \left(M_{\text{edge}} + B_c \cdot \int_0^{L_c} \int_0^{H} \rho \cdot \Phi(z, y) \cdot \mathrm{d}z \cdot \mathrm{d}y \right) \end{aligned} \tag{4b}$$

$$\begin{aligned} K^*_{\text{tot}} &= 1/2K_{\text{bent}} + \alpha_1^2 \cdot (K_{\text{abut}} + K_{\text{emb}}) + (1 - a_1)^2 K_{\text{deck}} \\ &= 1/2K_{\text{bent}} + (1 - a_1)^2 K_{\text{deck}} + a_1^2 \cdot \Bigg[K_{\text{abut}} - G \cdot B_c \\ &\quad \times \left(\int_0^{L_c} \int_0^{H} \Phi(z, y) \cdot \frac{\mathrm{d}^2 \Phi(z, y)}{\mathrm{d}z^2} \cdot \mathrm{d}z \cdot \mathrm{d}y + \int_0^{L_c} \int_0^{H} \Phi(z, y) \cdot \frac{\mathrm{d}^2 \Phi(z, y)}{\mathrm{d}y^2} \cdot \mathrm{d}z \cdot \mathrm{d}y \right) \Bigg] \end{aligned} \tag{4c}$$

where, B_c is the embankment average width, and G the embankment soil average shear modulus. These properties along with the damping coefficient $C^*_{\text{tot}} = a_1^2 \cdot C_{\text{emb}}$ (note that the embankment contribution is considered a major source of damping), are used to formulate the equation of motion of the generalized ESDOF system representing the embankment substructure:

$$M^*_{\text{tot}} \cdot \ddot{Y}(t) + C^*_{\text{tot}} \cdot \dot{Y}(t) + K^*_{\text{tot}} \cdot Y(t) = -M^*_{\text{tot}} \cdot \frac{\Im^*_{\text{tot}}}{M^*_{\text{tot}}} \cdot \ddot{u}_g \tag{5}$$

where $Y(t)$ is the response amplitude of the reference node and M^*_{tot} is the generalized mass of the embankment substructure. From (5) it follows that the response $Y(t)$ is calculated for a ground acceleration record scaled by parameter $\Im^*_{\text{tot}}/M^*_{\text{tot}}$ (alternatively if a spectral approach is used, accelerations, velocities, and displacements obtained from the spectrum are to be divided by the same parameter).

Terms $m_1 = 1/2M_{\text{center}} + \alpha_1^2 \cdot M_{\text{edge}}$ and $K_1 = [1/2K_{\text{bent}} + \alpha_1^2 \cdot K_{\text{abut}} + (1 - a_1)^2 K_{\text{deck}}]$ represent the mass and stiffness contribution of the bridge deck, attached on the embankment–deck contact node, with coordinates $(y, z) = (0, 0)$ (embankment model of Fig. 2). During analysis of the entire system, the central bent coordinate is considered as the reference node. For typical highway overcrossings with flexible bents and abutments, the fundamental mode of vibration of the embankment is: $\Phi(z, y) = \cos(z \cdot \sqrt{-\mu}) \cdot (e^{y\sqrt{\lambda}} + e^{2L_c\sqrt{\lambda}} \cdot e^{-y\sqrt{\lambda}})/(1 + e^{2L_c\sqrt{\lambda}})$, where the coefficients λ, μ are evaluated analytically (Kotsoglou and Pantazopoulou 2007a). In the present work, the dynamic response of the embankment model is evaluated by solving (5) in time, using standard time integration techniques. The result obtained for the response of the reference node is then correlated with the response obtained for the same reference point but from the other substructure assembly of the bridge idealization, comprising the abutments, bent and pile foundations (Fig. 2). Thus, the responses of the two substructures referring their point of contact are correlated through an iterative process in order to attain compatible displacement time histories at that interacting degree of freedom. In this process, the model of the embankment substructure is evaluated first, based on realistic assumptions for the superstructure properties attached to the embankment–deck contact node (Kotsoglou and Pantazopoulou 2007a). Then the deck–pier–abutment substructure model is re-calculated using the simplified frame representation of Fig. 2, with the embankment properties that were estimated in the previous step being attached to the embankment–deck contact node in order to verify the initial assumptions made. Note that a primary result of this analysis segment, which is of particular importance for the relevance of the successive iteration cycle, is the estimation of the shape of transverse vibration of the deck and in particular the ratio of displacement at the contact node, to that of the center of mass, a_1. This is needed in order to estimate the work-equivalent properties for the lumped mass and spring which are attached at the embankment–abutment contact point in order to represent the impedances imposed by the bridge–substructure on the embankment model. Another important ingredient for the same purpose is the pushover curve of all individual participating components of the deck–bent–abutment system wherever inelasticity is expected to occur, such as the central bent and the abutment pile foundation sub-system. Secant-to-yield stiffness values are initially assumed to represent each substructure. Furthermore in the deck–bent–abutments substructure assembly, properties of the lumped elements at the contact node are estimated from the embankment terms of Eq. 4:

$$K_{\text{emb}} = a_1^2 \cdot \left[-G \cdot B_c \cdot \left(\int_0^{L_c} \int_0^{H} \Phi(z, y) \cdot \frac{\mathrm{d}^2\Phi(z, y)}{\mathrm{d}z^2} \cdot \mathrm{d}z \cdot \mathrm{d}y + \int_0^{L_c} \int_0^{H} \Phi(z, y) \cdot \frac{\mathrm{d}^2\Phi(z, y)}{\mathrm{d}y^2} \cdot \mathrm{d}z \cdot \mathrm{d}y \right) \right],$$

$$C^*_{\text{tot}} = a_1^2 \cdot C_{\text{emb}} M_{\text{emb}} = a_1^2 \cdot B_c \cdot \int_0^{L_c} \int_0^{H} \rho \cdot \Phi^2(z, y) \cdot \mathrm{d}z \cdot \mathrm{d}y$$

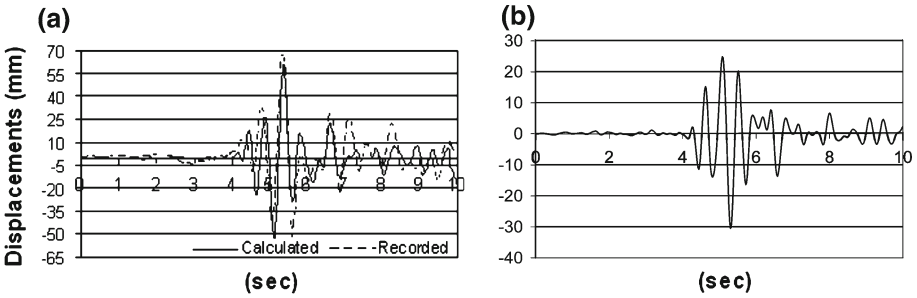

Fig. 4 **a** Evaluated and recorded dynamic response of the PSO during the 1992 Petrolia, Cape Mendocino main event, considering bridge–embankment interaction and **b** Calculated response obtained from conventional model without considering SSI effects (note the scale difference between (4a) and (4b))

4 Application to instrumented U.S. highway overcrossings

The model is used to calculate the dynamic responses of two well documented U.S. highway two-span bridges located in California, known in international literature as the PSO (for Painter Street Overcrossing) and the MRO (for Meloland Road Overcrossing). Both bridges are located in high seismicity regions near major faults and were instrumented as part of the California Strong Motion Instrumentation Program (CSMIP) in 1977. Since then, a significant database has been assembled from recorded responses during strong or moderate intensity excitations. Additional information regarding the geometry and material properties is provided elsewhere (Wissawapaisal 1999).

4.1 Dynamic response of the PSO during the Petrolia, Cape Mendocino Earthquake, 1992

The PSO is a prestressed concrete box-girder bridge (located in Rio Dell, California) having two spans of 44.5 and 36.3 m, supported on end abutments that are monolithically connected to the deck and a two column central bent. Both abutments and the central bent rest on driven concrete friction piles and are skewed at an angle of 39 degrees measured from the transverse direction. In 1992, the bridge was subjected to the Cape Mendocino, Petrolia Earthquake. Based on the recorded free-field accelerations, extensive analytical studies were conducted using the proposed model (Kotsoglou and Pantazopoulou 2007a) and displacement time histories of the entire bridge were evaluated providing excellent agreement with recorded responses (Fig. 4a). For the ground excitation intensity level under examination, the convergent value for the soil shear modulus G was 8 MPa and the corresponding modal damping value ξ was 26%. The estimated embankment critical length value was $L_c \approx 11$ m. The PSO response estimated with conventional modeling procedures that neglect bridge–embankment interaction effects is also plotted in Fig. 4b. Standard $P-x$ and $F-z$ horizontal and vertical soil–pile springs were utilized based on the soil properties, while the adopted modal damping value during analysis was 5%. Evidently, neglecting bridge–embankment interaction effects leads to significantly underestimated displacement demands. This, from an assessment perspective, is rather unconservative.

4.2 Dynamic response of the MRO during the Imperial Valley Earthquake, 1979

The MRO is a concrete box-girder bridge having two equal spans of 31.7 m, supported on end abutments monolithically connected to the deck and a single-column central bent. Both

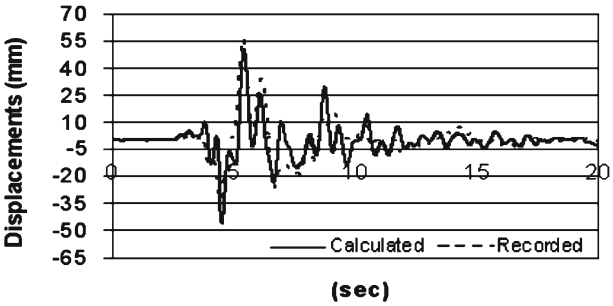

Fig. 5 Evaluated and recorded dynamic response of the MRO during the 1979 Imperial Valley main event, considering bridge–embankment interaction

abutments and the central bent rest on driven timber piles. The bridge is located near El Centro, California and in 1979 was subjected to the Imperial Valley Earthquake. Along the same line with the PSO, based on the recorded free-field accelerations, extensive analytical studies were conducted implementing the proposed model. Despite the satisfactory convergence between alternative models for the case of the PSO, significant variations are found in the literature between different investigations, regarding the estimation of the initial soil shear modulus $G_{\max}$ for the MRO. Conflicting initial soil shear modulus values are reported ranging from 19.4 MPa (Zhang and Makris 2002a) to 77MPa (Price and Eberhard 1998). From calibration of analysis with field records, Inel (2001) suggested a value of 43.2 MPa in order to provide compatible results with recorded responses. In the present study, from calibration of calculated results obtained with the model for the Imperial Valley 1979 strong motion record, very good agreement with recorded responses was found for $G_{\max} = 35$ MPa (Fig. 5). From implementation of the proposed analytical model (Kotsoglou and Pantazopoulou 2007a), the convergent value for the degraded soil shear modulus G was 3.8 MPa and the corresponding modal damping value ξ was 26%. Furthermore, the critical length value was estimated at $L_c \approx 9$ m.

5 Capacity curve evaluation

To use the proposed modeling procedure with established displacement-based seismic assessment methods, an adequate representation of the system's Capacity curve is required. Although in ordinary structures a conventional Pushover Analysis is appropriate, in case of highway overcrossings, significant uncertainties may be introduced due to the considerable modification of the system's dynamic characteristics as a result of ground excitation intensity. Increasing embankment mobilization during strong intensity ground excitations and the soil degradation under increased shear deformation levels, are identified as major sources of this irregularity. Therefore, in studying the dynamic response of approach embankments, contributing factors such as the degree of soil mobilization (described by the term "critical length L_c"), the stiffness and the deformation shape, may vary significantly during the response of the system. Under these circumstances, even well known conventional force reduction factors (*R-factors*) that are used widely for seismic assessment may not be applicable.

In the present study, an adaptive capacity curve of an ESDOF bridge–embankment approximation is defined, that incorporates the variation of the system's dynamic characteristics under different performance levels. Calculations are performed using Incremental Dynamic

Analysis—IDA (Vamvatsikos and Cornell 2004). Thus, to define the dynamic characteristics of the system and the capacity curve, equivalent elastic analysis is conducted iteratively for a wide range of earthquake intensity levels. (Iteration is needed so that the level of deformation demand attained at maximum response is compatible with the assumed degraded material moduli). Earthquake intensity is controlled by scaling up or down a set of representative accelerograms so as to attain different levels of peak acceleration. Note that within the context of analysis of the systems' resistance, IDA enables comparison of bridge responses to different ground motion records at the same level of peak acceleration as well as calculation of the pushover curve without requiring prior assumptions as to the pattern of applied forces; however, from a seismological perspective, there are objections to scaling down strong motion records in order to represent low intensity ground motions, as such an approach overlooks the differences in frequency content that characterize low intensity from large intensity ground motions.

For every level of ground acceleration considered, the critical embankment length L_c and the dynamic characteristics of the corresponding ESDOF system are evaluated after convergence of the iteration, and therefore the dynamic response of the entire bridge system is determined based on the proposed simplified deck model. The capacity curve of the system is generated from the evaluated pairs of peak "Force-Displacement" values (total base shear vs central bent relative displacement at the top) (Kotsoglou and Pantazopoulou 2007a,b). Separate pushover analysis was conducted in order to obtain the resistance curve of the bent-columns substructure (Fig. 6). Since the embankment–abutment system and the pier–bents function as springs in parallel in resisting the lateral motion of the superstructure, with the bent being usually the weakest mechanism, it is assumed that the ultimate displacement capacity of the overall system is controlled by this particular substructure. During design, the assumption of fixed base support for the bent columns yields conservative estimates of force demands. In the present case however, force resistance is not the main objective; rather, central bent columns need be designed to undertake the displacement demands of the entire bridge system. Here it is of great interest to investigate the actual seismic performance of the PSO bent, based on a simplified approach (more sophisticated modeling approaches may be found elsewhere (Mylonakis et al. 1997)). According to the geotechnical investigation (Heuze and Swift 1991), the soil profile at the location of the bent, consists of moderately compacted layers, with clayey silt and sand, silty sand with clay, sandy silt with clay and a very stiff brown clayey fine sand stratum. The underlying stratum consists of very dense gravelly, silty sand. From the above it is concluded that the undrained soil shear strength is ranging between 25 and 400 KPa depending on the soil stratum of interest.

A frame model is used in order to conduct the pushover analysis of the central bent (Fig. 6). Beam-column elements were used for the simulation of the bent columns, while appropriate plastic hinges were applied at each element node based on the moment curvature diagram of the column cross section (Fig. 7). Soil horizontal and vertical impedances acting on the pile foundation were represented through the use of appropriate $P-x$ and $F-z$ springs. Standard $P-x$ spring values may be derived based on the well known soil subgrade reaction modulus K_o, as a function of the soil type and depth (Bowles 1996), whereas $F-z$ springs representing the soil–pile contact (skin) resistance f_s, were evaluated based on the Tomlinson (1971) method. The total capacity of each pile group is estimated introducing the simplifying, well known Converse-Labarre (Bowles 1996) group efficiency coefficient, ($E_g \approx 0.62$), for friction piles. The resistance of the surface contact (skin resistance) is given by:

$$f_s = a_{\text{adh}} \cdot c + \bar{q} \cdot K_{\text{lat}} \cdot \tan\delta \tag{6}$$

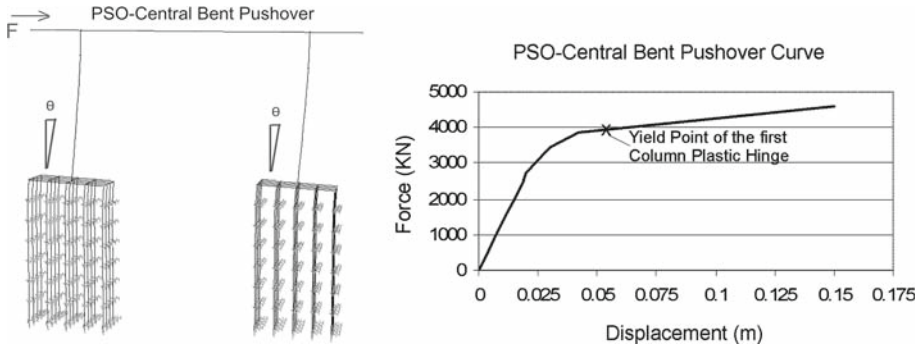

Fig. 6 PSO central bent capacity curve evaluation accounting also for soil–pile interaction

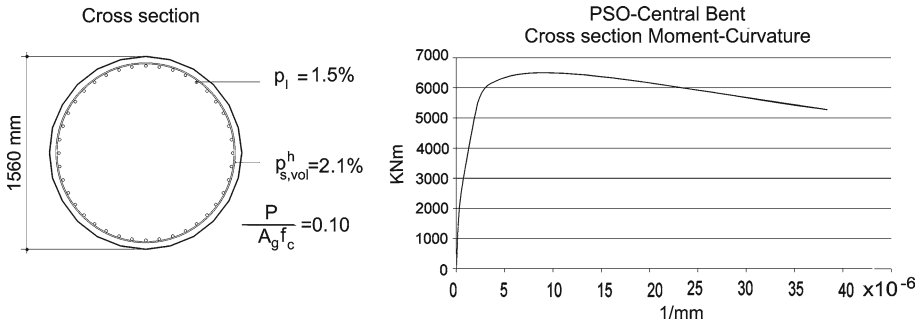

Fig. 7 Bent-column Moment-Curvature diagram of a typical California Overpass

where a_{adh} is the adhesion factor, c is the average cohesion (or s_u the undrained shear strength) for the stratum of interest, $\bar{q}$ is the effective stress, K_{lat} is the coefficient of lateral earth pressure and $\tan\delta$ the effective friction angle.

Based on the above, the ultimate surface pile capacity is evaluated approximately equal to $P_s \approx 400KN$. In order to account for the surface friction impedances, vertical $F-z$ inelastic springs were also attached on the model of Fig. 6. The ultimate $F-z$ spring force is considered to be fully utilized at a pile displacement of $0.05D$. The pushover curve of the entire bent is also plotted in Fig. 6. On the plot the estimated first yield of the concrete bent column is marked, indicating that the first plastic hinge is formed at a bent displacement value of 60 mm. Considering that the bent column yield displacement for the case of fixed supports is approximately 23 mm, it is concluded that the bent columns during the Petrolia Earthquake remained essentially elastic owing to the soil compliance and rotation of the foundation. This conclusion is in agreement with the field observations after the earthquake but also with studies by other investigators (Goel and Chopra 1997). The soil structure interaction altered dramatically the expected seismic performance by alleviating the flexural rotation demands of the column. It should be emphasized that in case of fixed support conditions, the displacement demands of the entire system are expected to be undertaken by the reinforced concrete columns. Therefore during design, it is realistic to recommend detailing of the bent columns based on the assumption of fixed supports (Inel and Aschheim 2004). Explicit models for the estimation of column rotation capacity may be used for assessment (Panagiotakos and Fardis 2001) (here, ultimate displacement capacity of the bent substructure is associated with loss of lateral load resistance). Based on tests it appears that the vertical load carrying capacity

Table 1 Imposed Ground Motion Records, [Mw = Magnitude, MF = Magnification Factor]

Ground-motion	MF	Date	PGA (g)	M_w	Geologic Fault Type/Comments
USA_Petrolia	1.0	25/4/1992	0.472	6.4	–
Japan_Kobe-Takatori	1.0	16/1/1995	0.616	6.9	Near fault-Strike slip
Japan-(EW) Off Iwate Pref.	1.0	6/12/1968	0.167	7.2	Strike-slip
Japan-(NS) Off Iwate Pref.	1.0	6/12/1968	0.195	7.2	Strike-slip
Japan-(EW) Off Iwate Pref.	3.0	6/12/1968	0.501	–	Strike-slip
Japan-(NS) Off Iwate Pref.	3.0	6/12/1968	0.585	–	Strike-slip
IRA-A	1.0	–	0.453	7.8	Strike-slip with a thrust component
IRA-B	1.0	–	0.351	7.8	Strike-slip with a thrust component
IRA-C	1.0	–	0.552	7.8	Strike-slip with a thrust component

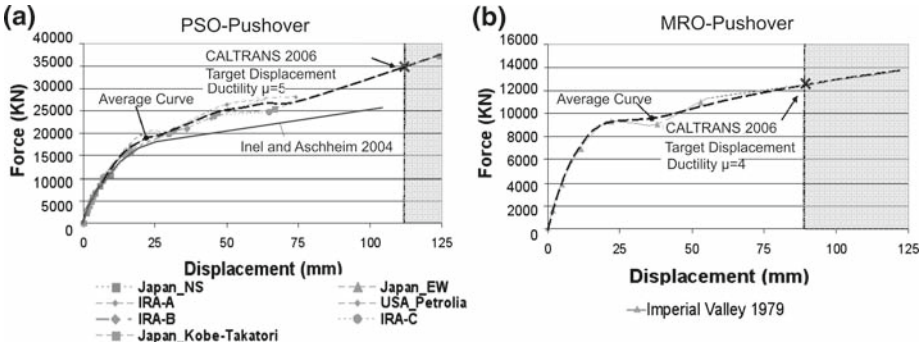

Fig. 8 Pushover Curve Estimation implementing the proposed method **a** PSO and **b** MRO

of the system is significantly impaired past that point (Elwood and Moehle 2004). For this reason, exceedance of the ultimate displacement capacity of the bent is identified as failure for the system. Target displacement demands provided by bridge codes may be used in pier design (CALTRANS 2006), (for example, current CALTRANS (2006) provisions, suggest target displacement ductility for single column bents and for multi-column bents equal to $\mu_d = 4$ and $\mu_d = 5$, respectively).

An objective of the present section is to evaluate the capacity curves of the entire bridge–embankment system. Again, here the well documented PSO and MRO records are used as benchmark and the capacity curves of these systems were evaluated by implementing the proposed procedure. A considerable number of characteristic ground-motions were used during analyses in order to cover a wide range of expected excitations. Some major ground-motions that were used among others for the evaluation of the PSO Capacity Curve are listed in Table 1. The Japan_Kobe-Takatori record is considered a representative near-fault excitation while the Japan-EW and Japan-NS events are records with unusually high frequency in the major loading cycles (Japan-Off Iwate Pref 1968). Additionally, the use of an artificially generated accelerogram set, corresponding to a strike-slip fault with a thrust component would be relevant (IRA-A, IRA-B, IRA-C), (Mori and Crouse 1981; Papazachos 1996; Theodulidis 2002). Generated capacity curves of the PSO and the MRO are plotted in Fig. 8a and b in terms of base shear vs. central bent displacement, based on convergent soil shear strains for the embankments.

A set of "Force-Displacement" pairs is obtained in response to the various records. A single representative capacity curve is then drawn as the statistical average of the available sample. Results are shown for the two bridges by the dashed trend lines in Fig. 8a and b and are used in the remainder for demonstration of the intended method of seismic assessment. Also plotted in Fig. 8a is the pushover curve for the PSO provided by Inel and Aschheim (2004), obtained after estimation of the effective embankment length through calibration of calculated with recorded responses. Pushover curves obtained from the two approaches for the PSO system are in good agreement with consistent estimates for the yield displacement of the entire system. Significant strain-hardening is obtained in both cases considered, owing to the stabilization of the $G/G_{\max}$ ratio to an almost constant residual value for very large strains following the abrupt degradation from the peak. Thus, at that stage of response, the embankment system participates to the response almost through constant kinematic impedances as a function of the embankment critical length. Also plotted in Fig. 8a and b are the target displacement ductility demands estimated according to CALTRANS (2006) for the conservative case of stiff pile–foundation (fixed supports).

Estimation of the critical embankment length is considered an important step, since this variable quantifies the mobilization of the embankments to the bridge response. Increased embankment length, leads to significant post-elastic stiffness for the entire bridge–embankment system.

6 Displacement based assessment

Given the capacity curve of the ESDOF approximation of the entire bridge system also accounting for soil–structure interaction, familiar methods to estimate the system's performance are applicable (e.g. the "Capacity Spectrum" method (Fajfar 1999), the "N2" method (Fajfar 2000) and the "Yield Point Spectra" method Aschheim and Black 2000). In all cases mentioned, the performance point (i.e. the anticipated displacement and force demand under a given seismic hazard) is determined by superimposing the capacity curve (properly scaled bilinear approximation through use of the equal area rule) on the response spectrum of the design hazard (eg. design spectra, or any ground motion spectra drawn in ADRS format, either elastic with high damping when using the capacity-spectrum approach, or isoductile Yield Point Spectra, when using the YPS approach, Fig. 9). For simplicity, the Newmark and Hall (1973) $R-\mu-T$ relationships were used to construct the YPS Spectra. For compatible units, the capacity curve is normalized with respect to weight. In the problem considered, where the degree of embankment mobilization depends on the level of earthquake intensity, the resulting modifications of the generalized mass of the ESDOF according with Eq. 2 should be also considered.

Displacement demands for the PSO and the MRO are estimated under a wide range of actual earthquake excitation events recorded in California (Fig. 10). A general design and assessment procedure for highway overcrossings using the YPS is as follows:

- Based on the seismicity of the bridge region select an adequate number of representative ground-motions (intensity, duration, fault type, distance from the epicenter, etc).
- Through IDA of the generalized ESDOF representation of the bridge–embankment system (Eq. 2) evaluate the pushover curve of the entire system, and consistently convert to a bilinear statistical average curve. In defining the knee point in the bilinear curve, owing to the significant strain hardening that characterizes embankment participation under large strains, the equal-areas rule should be used.

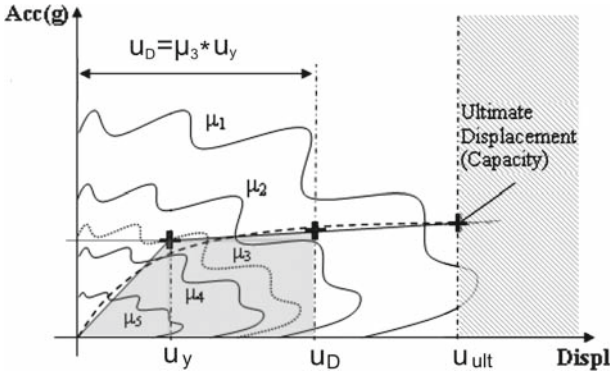

Fig. 9 The Yield Point Spectra-YPS method (Aschheim and Black 2000)

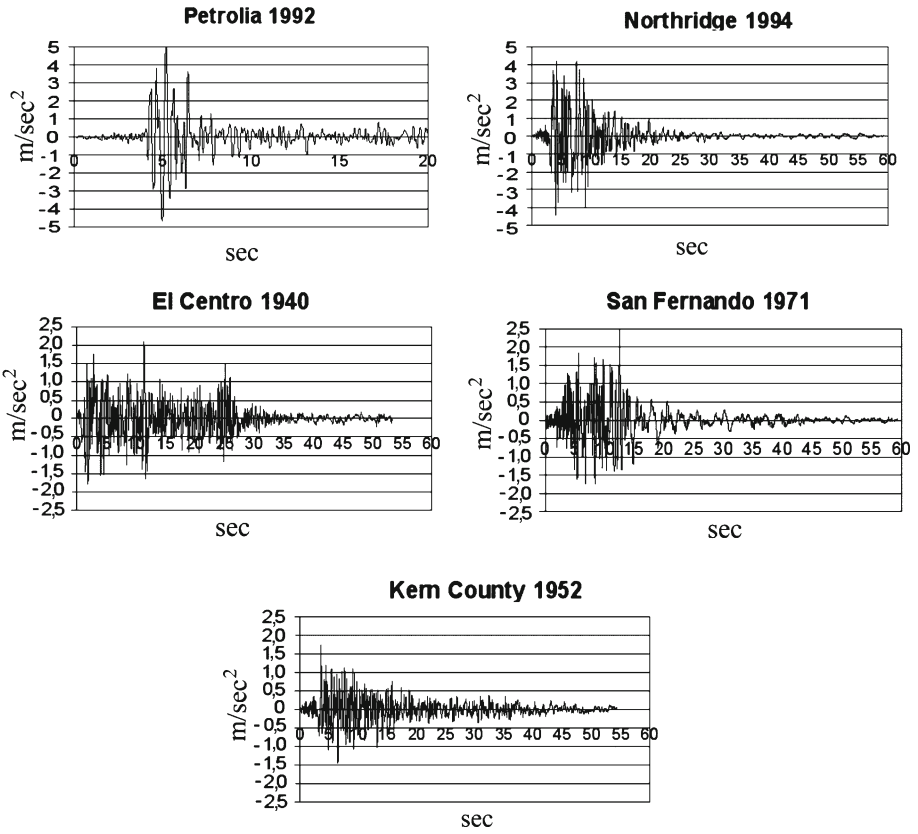

Fig. 10 Imposed excitations considered in application of the proposed model to the PSO and MRO examples

- The apparent yield force and associated displacement characterize the entire bridge–foundation–embankment system. In this context, the "yield" point is the point of abrupt slope change in the approximated bilinear pushover curve, and thus, it may correspond to a displacement level past the occurrence of significant nonlinear events in some of the

individual components of the system (possible sources of nonlinearity are the rotation of the foundation support due to soil compliance, embankment soil degradation, and yielding of the piers). This method of defining an apparent yield point is meaningful for bridge–embankment systems with significant post-elastic stiffness.

- Based on the elastic branch of the bilinear curve and the estimated yield displacement, evaluate the corresponding soil shear strain γ and therefore the damping ξ using appropriate "damping-shear strain" curves provided in the literature for a wide range of soil types (AASHTO-83 1988; Iwasaki et al. 1978; Tatsuoka et al. 1978; Vucetic and Dobry 1991; Seed and Idriss 1970).
- Obtain the bundle of YPS curves for any ground-motion spectrum that describes the reference seismic hazard for various ductility levels. For simplicity well known $R-\mu-T$ relationships are used (eg. Newmark and Hall 1973). Damping is provided from the previous step.
- Scale the pushover curve (as described in Sect. 6.1) and evaluate the seismic demands in terms of displacement ductility by plotting the scaled pushover curve on the YPS system of coordinates, as explained in Sect. 6.1 (Fig. 9).

6.1 ESDOF transformation

Equation 2 is developed further as follows:

$$\begin{aligned}&\lfloor 1/2M_{\text{center}} + \alpha_1^2 \cdot (M_{\text{edge}} + M_{\text{emb}}) \rfloor \cdot \ddot{u}_1 + C_{\text{emb}} \cdot a_1^2 \cdot \dot{u}_1 \\ &+ \lfloor 1/2K_{\text{bent}} + \alpha_1^2 \cdot (K_{\text{emb}} + K_{\text{abut}}) + (1-a_1)^2 K_{\text{deck}} \rfloor \cdot u_1 \\ &= -\frac{\lfloor 1/2M_{\text{center}} + a_1 \cdot (M_{\text{edge}} + M_{\text{emb}}) \rfloor}{[1/2M_{\text{center}} + \alpha_1^2 \cdot (M_{\text{edge}} + M_{\text{emb}})]} \cdot [1/2M_{\text{center}} + \alpha_1^2 \cdot (M_{\text{edge}} + M_{\text{emb}})] \cdot \ddot{u}_g\end{aligned} \tag{7}$$

Considering that $\lfloor 1/2M_{\text{center}} + a_1^2 \cdot (M_{\text{edge}} + M_{\text{emb}}) \rfloor$ is the generalized mass of the system, accelerations, damping and displacements obtained are divided by parameter $\alpha = \frac{\lfloor 1/2M_{\text{center}} + a_1 \cdot (M_{\text{edge}} + M_{\text{emb}}) \rfloor}{[1/2M_{\text{center}} + \alpha_1^2 \cdot (M_{\text{edge}} + M_{\text{emb}})]}$.

Therefore, forces and displacements provided by the initially evaluated pushover curve are normalized by parameter a prior to superposition on the YPS. From the above, it can be observed that the parameter a of a certain system may vary for different imposed ground acceleration intensities owing to the expected modification of its dynamic properties. Nevertheless, average values of this parameter may be adopted in case of systems that are characterized by the same order of evaluated contributing modal mass values under successively increasing earthquake loads (eg. PSO and MRO). The method is used to evaluate the response of the PSO and the MRO under a suite of five different ground motions recorded in California (Fig. 10). Estimated ductility demands are obtained as per Fig. 11 using the YPS method for the five strong motion spectra. Estimated maximum displacements for the transformed ESDOF approximation (u_{SDOF}) and also for the entire bridge system (u_{Global}) are summarized in Table 2. Generalized mass for the two overcrossings was found approximately constant and therefore a single value of the parameter a is used for both cases without introducing considerable errors to the analysis.

As shown in Table 2, the PSO and MRO behavior under seismic accelerations of $0.15 \div 0.20$ g (i.e. San Fernando 1971, El Centro 1940 and Kern County 1952 records depicted in Fig. 10) is considered essentially elastic as the induced low soil shear strain levels imply stiff embankment response. Under strong intensity ground excitations ($0.40 \div 0.50$ g, i.e.

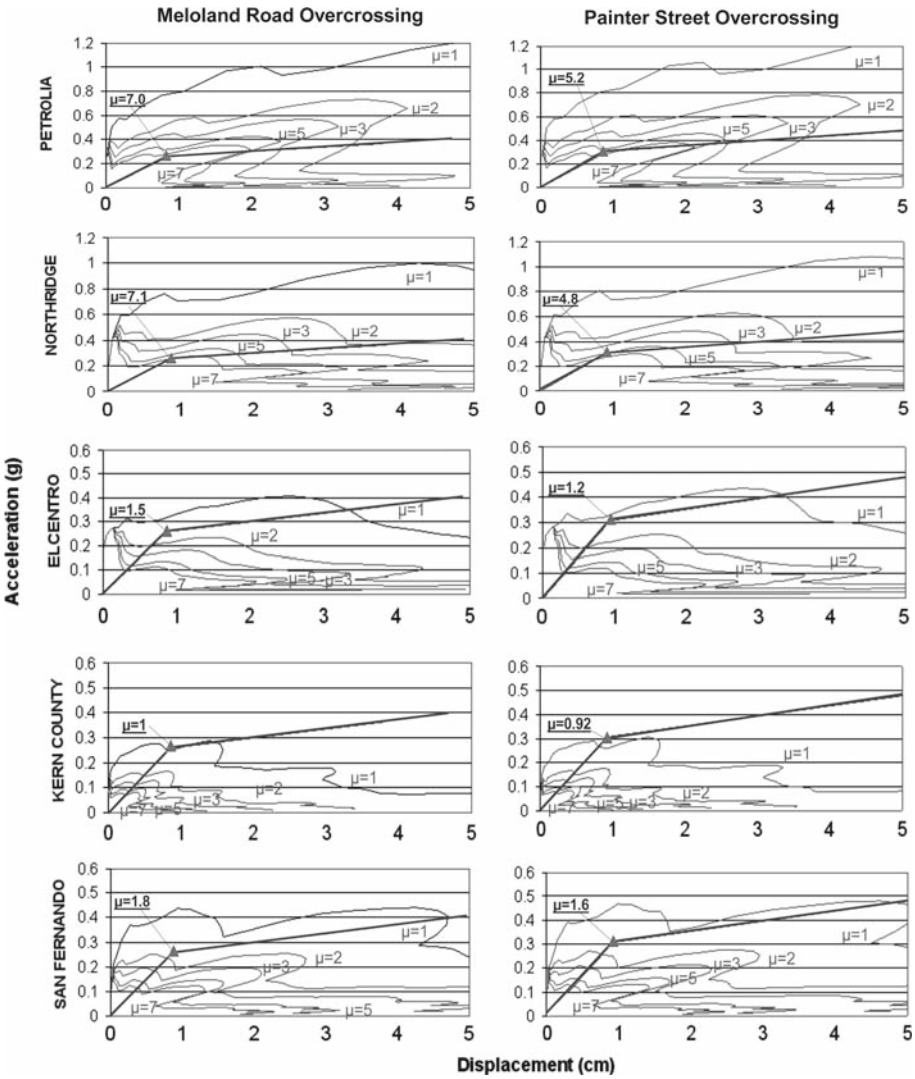

Fig. 11 Yield Point Spectra method implementation for the PSO $\xi = 13\%$ and the MRO $\xi = 15\%$ bridge–embankment systems

Table 2 Estimated displacement demands of the MRO and the PSO bridge–embankment system

Ground-motion	MRO: $\alpha = 1.39$ and $u_{y,\mathrm{SDOF}} = 8.63$ mm			PSO: $\alpha = 1.35$ and $u_{y,\mathrm{SDOF}} = 9.25$ mm		
	μ_d	$u_{D,\mathrm{SDOF}}$(mm)	$u_{D,\mathrm{Global}}$(mm)	μ_d	$u_{D,\mathrm{SDOF}}$ (mm)	$u_{D,\mathrm{Global}}$(mm)
Petrolia	7.0	60.41	83.97	5.2	48.1	64.94
Northridge	7.1	61.27	85.16	4.8	44.4	59.94
El Centro	1.5	12.95	17.99	1.2	11.1	14.99
Kern County	1.0	8.63	12.00	0.92	8.51	11.49
San Fernando	1.8	15.54	21.60	1.6	14.8	19.98

Petrolia 1992 and Northridge 1994 records depicted in Fig. 10) the soil-shear modulus degradation introduces significant nonlinearities to the global response. From the above analytical results, the influence of the frequency content of the imposed ground-motion should be underscored, as moderate acceleration amplitudes (≈ 0.25 g) may introduce excessive displacement demands in case of near fault excitations (Fig. 5-Imperial Valley 1979).

Furthermore, since the initial soil shear modulus $G_{\max}$ of the MRO (34 MPa) embankment is considerably lower as compared to that of the PSO (60 MPa), the MRO response is expected to be marked by increased soil shear strains under significant excitations. These trends are confirmed by the results listed in Table 2. The MRO bridge–embankment response corresponds to increased displacements under significant imposed accelerations (i.e. Cape-Mendocino, Petrolia 1992 and Northridge 1994 earthquakes). Therefore, global displacement ductility demands of 7.0 (Petrolia 1992) and 7.1 (Northridge 1994) were estimated for the MRO under strong intensity excitations, while the global displacement ductility demands for the PSO were estimated as 5.2 (Petrolia 1992) and 4.8 (Northridge 1994). Yield displacement for both studied bridge–embankment ESDOF systems was found in the range of $u_y \approx 0.1\%H$. According to Fig. 11 and with respect to Table 2, peak accelerations for the global bridge–embankment system during the Petrolia earthquake for the PSO were estimated as 0.75 g. Acceleration estimations of the PSO deck based on the proposed procedure (Fig. 11), are in good agreement with the recorded response at the PSO central bent (≈ 0.75 g) reported by Inel (2001). Significant seismic demands in terms of central bent displacements were identified during the Cape Mendocino/Petrolia and Northridge records due to the bridge–embankment interaction and embankment flexibility under increased soil shear strains. The seismic performance of the central bent–pile foundation system is considered of critical importance, as the soil–pile–foundation response determines the behavior of the bent-columns. Therefore, in case of fixed column supports, significant column displacement ductility demands are anticipated with $\mu_d \geq 2.5 \div 3$ for the PSO and the MRO, respectively, during the Petrolia 1992 and the Northridge 1994 earthquakes, whereas for piers with a compliant foundation system, nonlinear behavior is expected to occur in the foundation past the elastic limit.

As discussed earlier and also shown in Table 2, it is emphasized that the estimated yield displacements corresponding to the global bridge–embankment system when accounting for soil–structure interaction, differ significantly from those obtained when considering yielding of the central bent column alone. The bridge–embankment system is performing inelastically while the bent columns and the deck remain elastic. This kind of response is attributed to the embankment inelastic behavior and the degradation of the soil shear modulus under significant soil shear strains. Therefore it is evident that the implementation of $R - \mu - T$ relationships in the case of integral bridges with embankment mobilization is only valid when used through implementation of methods that account for the bridge–embankment interaction, such as those presented in this paper.

7 Conclusions

Soil–structure interaction is a factor of critical importance during design and assessment of integral R.C. bridges. Recent results indicate that embankment flexibility and soil mobilization under strong intensity ground excitation may considerably affect the seismic performance of the entire system and may result in increased displacement demands in the ductility controlled structural elements (such as bridge piers). In the present paper, an explicit procedure is developed, based on proposed modeling and analysis approaches and also on established

design and assessment methods. A basic step of the method is transformation of the entire bridge–foundation–embankment system to a generalized ESDOF. Through application of this model and consistent linearization of system's properties, the capacity curve of the system is evaluated with Incremental Dynamic Analysis-IDA. Demands for bridge assessment to a specific design hazard are established using the YPS approach on the ADRS spectrum.

Extensive studies were conducted for two well-documented U.S. overcrossings, the PSO and the MRO. Significant hardening in the post-elastic branch of the entire system's push-over curve owing to the embankment contribution was identified in both case studies used for verification. Seismic demands were calculated for a wide range of acceleration records, highlighting the excessive displacements that may be imposed on bridge piers owing to mobilization of the embankments. Excessive displacement demands are also expected in case of near fault excitations with long period pulses (Imperial Valley 1979) even during moderate imposed accelerations. It is worth noting for comparison than conventional modeling of the bridges considered (by ignoring the bridge–embankment interaction effects), significantly underestimate the displacement demands.

Soil–pile interaction effects and foundation flexibility at the central bent are factors of critical importance controlling the extent of damage in the pier: foundation flexibility relieves the pier deformation required to develop the imposed displacement demands. For example, owing to soil compliance and soil–pile interaction the PSO bent columns remained elastic despite the significant displacement experienced by the deck during earthquake, but pullout slip of the piles exceeded the elastic limit of that group of elements, which in the context of design is considered a type of foundation failure; similarly, the situation of a stiff foundation system for the central pier would lead to excessive damage estimates for that element when the embankment compliance is considered, as the global effect of embankment mobilization generally is increased deck displacements. Thus, the need to detail the pier and pier–foundation system with displacement-based procedures when bridge–embankment interaction effects are anticipated cannot be overemphasized, particularly in the case of bridges supported on earth embankments.

Acknowledgments Research presented in this paper was funded by the Hellenic Secretariat for Research and Technology through the Research Consortium "ASPROGE".

References

AASHTO-83 (1988) Guide specifications for seismic design of highway bridges. American Association of State Highway and Transportation Officials, Washington

Aschheim M, Black E (2000) Yield point spectra for seismic design and rehabilitation. Earthq Spectra Earthq Eng Res Inst 16(2):317–335

Bowles J (1996) Foundation analysis and design. 5th edn. McGraw-Hill

CALTRANS (2006) CALTRANS seismic design criteria, version 1.4. California Department of Transportation, Sacramento, USA

Elwood K, Moehle J (2004) Evaluation of existing reinforced concrete columns, Proceedings, 13th World Conference on Earthquake Engineering, Vancouver

Fajfar P (1999) Capacity spectrum method based on inelastic demand spectra. Earthq Eng Struct Dyn 28(9):979–993

Fajfar P (2000) A nonlinear analysis method for performance-based seismic design. EERI Earthq Spectra 16(3):573–592

FEMA-274 (1997) NEHRP commentary on the guidelines for the seismic rehabilitation of buildings, report No. FEMA-274, Federal Emergency Management Agency, Washington, D.C., October 1997

Gazetas G (1987) Seismic response of earth dams: some recent developments. Soil Dyn Earthq Eng 6(1):3–47

Goel RK, Chopra AK (1997) Evaluation of bridge abutment capacity and stiffness during earthquakes. Earthq Spectra 13(1):1–23
Heuze FE, Swift RP (1991) Seismic refraction studies at the Painter Street Bridge site, Rio Dell, California. Report UCRL-ID-108595. Lawrence Livermore National Laboratory, Oak Ridge, TN
Inel M (2001) Displacement-based strategies for the performance-based seismic design of "short" bridges considering embankment flexibility. Thesis, University of Illinois at Urbana-Champaign
Inel M, Aschheim MA (2004) Seismic design of columns of short bridges accounting for embankment flexibility. J Struct Eng 130(10):1515–1528
Iwasaki T, Tatsuoka F, Takagi Y (1978) Shear moduli of sands under cyclic torsional shear loading. Soils Found 18(1):39–56
Kappos A, Potikas P, Sextos A (2007) Seismic assessment of an overpass bridge accounting for nonlinear material and soil response and varying boundary conditions, Computational methods in structural dynamics and earthquake engineering, COMPDYN 2007, Rethymnon, Greece
Kotsoglou A, Pantazopoulou S (2007a) Bridge–embankment interaction under transverse ground excitation. Earthq Eng Struct Dyn 36(12):1719–1740
Kotsoglou A, Pantazopoulou S (2007b) Soil–structure interaction: capacity curve evaluation and seismic assessment of highway overcrossings, 4th ICEGE-international conference on earthquake geotechnical engineering, Thessaloniki, Greece, 25–28 June 2007
Mackie K, Stojadinovic B (2003) Seismic demands for performance-based design of bridges. PEER Report 2003/16. Pacific Earthquake Engineering Research Center, University of California, Berkeley, CA
McCallen DB, Romstad KM (1994) Dynamic analysis of a skewed short-span, box-girder overpass. Earthq Spectra 10(4):729–755
Mori A, Crouse C (1981) Strong motion data from Japanese earthquakes, World Data Center for Solid Earth Geophysics, Report SE-29
Mylonakis G, Nikolaou A, Gazetas G (1997) Soil–pile–bridge seismic interaction: kinematic and inertial effects, part I: soft soil. Earthq Eng Struct Dyn 26(3):337–360
Newmark NM, Hall WJ (1973) Seismic design criteria for nuclear reactor facilities, building practices for disaster mitigation, Report Number 46, National Bureau of Standards, U.S. Department of Commerce, 209–236
Panagiotakos TB, Fardis MN (2001) Deformation of reinforced concrete members at yielding and ultimate. ACI Struct J 98(2):135–148
Papazachos B (1996) Large seismic faults in the Hellenic arc. Annali di Geofisica 39:891–903
Price TE, Eberhard MO (1998) Effects of spatially varying ground motions on short bridges. J Struct Eng 124(8):948–955
Priestley MJN, Seible F, Calvi GM (1996) Seismic design and retrofit of bridges. Wiley, New York
Seed HB, Idriss IM (1970) Soil moduli and damping factors for dynamic response analysis. Report Number EERC70-10, University of California, Berkeley, CA
Tatsuoka F, Iwasaki T, Takagi Y (1978) Hysteretic damping of sands under cyclic loading and its relation to shear modulus. Soils Found 18(2):25–40
Theodulidis N (2002) Strong motion simulation of large intermediate depth earthquakes in SE Europe, Proceedings of the 12th ECEE, paper Mo. 668 (on CD)
Tomlinson MJ (1971) Some effects of pile driving on skin friction. Proceedings, conference on behavior of piles, ICE, London, pp 107–114
Vamvatsikos D, Cornell CA (2004) Applying incremental dynamic analysis. Earthq Spectra 20(2):523–553
Vucetic M, Dobry R (1991) Effect of soil plasticity on cyclic response. J Geotech Eng, ASCE 117(1):89–107
Wilson JC, Tan BS (1990a) Bridge abutments: formulation of a simple model for earthquake response analysis. J Eng Mech 116(8):1828–1837
Wilson JC, Tan BS (1990b) Bridge abutments: assessing their influence on earthquake response of meloland road overpass. J Eng Mech 116(8):1838–1856
Wissawapaisal C (1999) Modelling the seismic response of short bridges. PhD Thesis, University of Illinois at Urbana-Champaign
Zhang J, Makris N (2001) Seismic response of highway overcrossings including soil–structure interaction. Report No: UCB/PEER 2001/02, University of California, Berkeley, February 2001
Zhang J, Makris N (2002a) Kinematic response functions and dynamic stiffnesses of bridge embankments. Earthq Eng Struct Dyn 31:1933–1966
Zhang J, Makris N (2002b) Seismic response analysis of highway overcrossings including soil–structure interaction. Earthq Eng Struct Dyn 31:1967–1991